J Incl Phenom Macrocycl Chem (2012) 74:211–221
DOI 10.1007/s10847-011-0102-8

ORIGINAL ARTICLE

Theoretical and experimental study of the tetracain/β-cyclodextrin inclusion complex

N. L. Chekirou · I. Benomrane · F. Lebsir · A. M. Krallafa

Received: 12 July 2011 / Accepted: 15 December 2011 / Published online: 28 January 2012

Abstract The local anaesthetic Tetracain has previously been found to block, induce or potentiate Ca^{2+} release from the sarcoplasmic reticulum of skeletal muscle. Cyclodextrins (CD) are complexing agents that have been successfully used as pharmaceutical drug carriers, to improve the bioavailability of medicines. The aim of this work is to investigate the inclusion process of the local anesthetic Tetracain with the beta-cyclodextrin at the Hartree–Fock level of theory calculations with a 6-31G (d) basis set, and to evaluate stabilization upon the formation of the inclusion compounds for 1:1 association. The inclusion process pathways are described and the most stable structures of the different complexes are sought through a global potential energy scan. The data suggest that the most stable structure for the **1**:**1** stoichiometry between the Tetracain and the β-CD is obtained when the inclusion complex formed by Tetracain from the tertiary amine group, entering into the cavity of β-CD from its narrow side (i.e. the primary 6-CH_2OH hydroxyl group). Structure–activity relationship is discussed in terms of different molecular descriptors and experimental Raman spectroscopy measurements at different mole fraction for the inclusion complexes analyzed and compared with our theoretical constructed Raman spectra.

Keywords Tetracain · β-Cyclodextrin · Quantum calculation · Inclusion process · Fukui functions · Raman spectroscopy

N. L. Chekirou · I. Benomrane · F. Lebsir · A. M. Krallafa (✉)
Laboratoire de Chimie Physique Macromoléculaire, Département de Chimie, Faculté des Sciences, Université d'Oran, B. P. 1524, Oran El-Menouar, Algeria
e-mail: krallafa.abdelghani@univ-oran.dz; a.krallafa@yahoo.fr

Introduction

In recent years, the method of molecular complexation with artificial receptors becomes more and more useful in several technological and research fields [1, 2]. Besides, highly specific biological processes make intensive use of molecular complexation, with noncovalent interactions playing an important role [3]. Most researchers working in the field of molecular recognition processes have focused on number of therapeutic molecules, whose bioavailability is often affected by problems such as limited solubility or stability. Recently, molecular encapsulation has been successfully used in several technological fields [3, 4]. Pharmaceutical industry has made use of the technique to improve the bioavailabilities of drugs, to protect them from decomposition, to convert liquids to free flowing powder, and to mask unfavorable odors and tastes. Inclusion complexation is the focus of current host–guest chemistry and supramolecular chemistry [5–7], as the use of CDs in pharmaceutical is due to their ability to enhance solubility and chemical stability of poorly soluble drugs, reduce toxicity and control the rate of release [8, 9]. Cyclodextrins (CDs), the most prominent host molecules up to date, which becomes a new family of pharmaceutical excipients, are cyclic oligosaccharides consisting of 6, 7, or 8 (α, β or γ cyclodextrins, respectively) glucose units connected by α-1,4-glycoside bonds [10], with a shape of truncated cone, having a hydrophobic cavity [10]. Several hydroxyl groups are located on the outer part of the ring, which make the CDs both hydrophilic and soluble in water. The unique ability of CDs to entrap some molecules in their molecular cavities offers remarkable effects in stabilizing and solubilizing lipophilic unstable substances without the formation of chemical bonds and without changing their structure, such physical interaction can be considered as

encapsulation of substances at a molecular scale [11, 12]. If such statement does apply for the host, it is far from being true for the guest molecule as it will be seen in the present work. Although, substantial structural changes of the guest molecule occur, no major changes on the activity are observed. Among this class of "host" molecule, β-cyclodextrin (β-CD) with seven glucose units is broadly used to enhance the solubility, stability and bioavailability of drugs [7, 13, 14] and is the favorite encapsulation of drugs in the pharmaceutical industry, for its lower price and higher productive rate [15]. The β-CD has a rather rigid structure and the intramolecular hydrogen bond formation is probably the explanation for the observation that β-CD has the lowest water solubility of all CDs [16].

Tetracain belongs to an important class of synthetic drugs of the therapeutic family of local anesthetics, whose structures resemble natural compounds actively participating in nerve impulse transmission. It is believed that the cationic form of the drug, which seems to be the active principle, joins the Na+ channels on the nerve membrane, thus blocking the initiation and transmission of nervous impulses [17–19]. However, local anesthetics often show a short duration of action, and adverse side effects, such as cardiac and neurological toxicity, accompanied sometimes by allergic reactions. It is then expected that the formulation of Tetracain hydrochloride as microencapsulate with a cyclodextrin may show a better bioavailability [20], with all or some of these undesirable effects masked or abolished.

Because of the limitation of the experimental methods, molecular modeling is very popular in CDs chemistry [21–29], and the quantum calculations seem to be the only route to achieve the search for the global minimum. However, such calculations are difficult to carry out because of the size of the molecular system. Over the past few years all attempts made to investigate such processes have focused mainly towards CD complexation which was performed at several starting points rather than over a global search of the potential energy surface of the inclusion process [31–33].

The aim of this work is to investigate the potential surface of the inclusion process of the Tetracain into the β-CD using the advanced semi empirical molecular orbital PM3 method [31] as a probing tool. This method is well known in the conformational study of some supramolecular systems [31, 33] and remains the more efficient approach for such large molecular systems when preliminary quantum calculations are required. Such relative faster and less time consuming method enable us to identify the different insertion tables observed in the complex formation. The resulting complexes observed are then studied at the HF level of theory with a 6–31g(d) basis set. A full analysis of the results is then performed from the chemical, thermodynamics and spectroscopic standpoints. Raman spectroscopy has previously been applied to the successful study of various pharmaceutical analyses [34–36], therapeutic, narcotic agents and polymer based drugs. For that purpose, we report a comparative Raman study between the theoretical and experimental spectra in order to identify specific host–guest complexes.

Computational details

In the following investigation, all calculations are performed with the Gaussian 03 program [37]. Considering the large number of atoms in the studied system, an adequate choice of the model chemistry had to inevitably result from a compromise between the available computer power and the desired level of calculation. The compromise is particularly important for full geometry optimization calculations, since these tasks are computationally expensive at the ab-initio level of theory for such large system. We have then chosen to use the PM3 approach to model the inclusion pathway of complexes. First, we start from optimised structures for the host and the guest molecule at high level of theory (HF/6-31G(d)), and the calculation of the inclusion process are performed with a full optimisation of every point and with the atoms of the β-CD frozen with the PM3 hamiltonian with the assumption that the guest molecule undergoes greater structural changes than the host molecule. In a second step, the identified minima of the potential energy profile, are taken and fully optimised by releasing all variables of the β-CD at higher level of theory (HF/6-31G(d)).

In order to examine in details the reaction pathways and seek for a possible global minimum, we proceeded as follows. The controlled reaction coordinate (Z) of the inclusion process is the distance between two dummy atoms, one located at the center of mass of the amine group in the Tetracain and the second is located right below the centre of the glycosidic oxygen atoms of the β-CD as illustrated in Fig. 1. Dummy atoms are kept frozen at their initial position throughout the calculation. This position ensures that the insertion coordinate is positive. All the possibilities of the inclusion process were considered: the orientation in which the Tetracain points toward the narrow side of the β-CD ring (primary face) and the other case in which the Tetracain points toward wider ring (secondary face).

Experimental

The Tetracain and the β-CD in a powder form were purchased from Sigma-Aldrich Chemical Company with a purity of 99% and it was used as such without further purification.

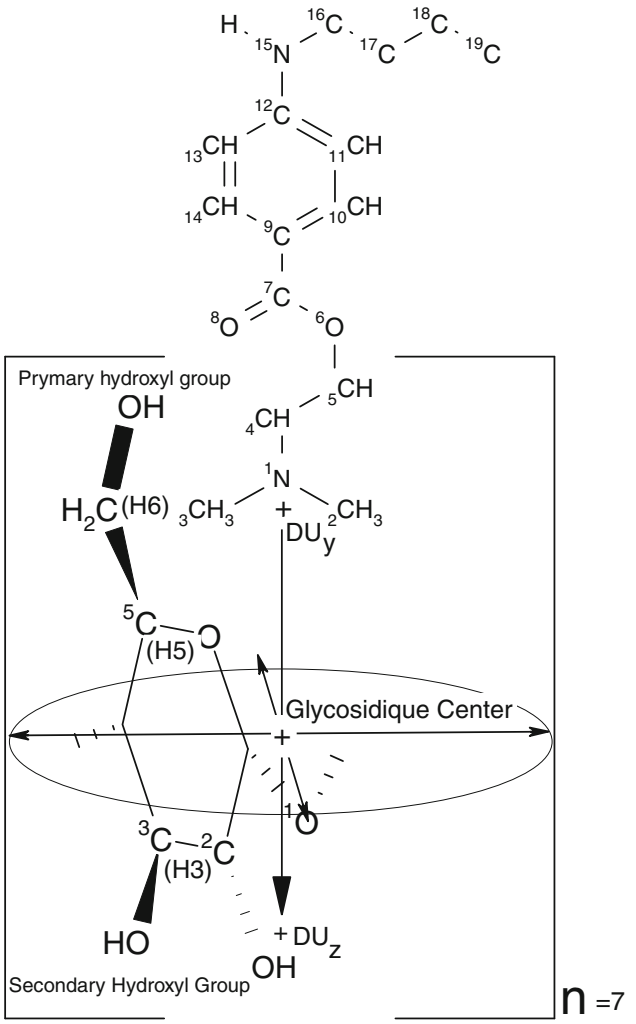

Fig. 1 Starting configuration of the inclusion process Tetracain/β-CD, (DU_y-DU_z) is the approaching distance between the two dummy atoms (to avoid negative values of the insertion coordinate, dummy atom DU_z is located below the center of the oxygen glycosidic rim). Atom labels are reported for identification of active sites in the Tetracain

High-Resolution Raman Spectra were collected on a Renishaw InVia Raman at the Laboratoire Condition Extrémes et Matériaux Haute Temperature et Irradiation. CEMHTI, CNRS Orleans, France. The Tetracain forms a meta-stable hydrate in the presence of water and this result in a depression at its melting point from 42 to 29 °C. The experimental spectra are obtained in aqueous solution at different mol fractions of the two components in the insertion process, starting from the same ratio of Tetracaine and β-CD (50%). In the first series the Tetracain is added in excess with a mol fraction ranging from $X_{Tetra} = 50.0$ to 100%. In the second series the β-CD is added in excess with a mol fraction ranging from $X_{\beta\text{-CD}} = 50.00\%$ up to 100%.

Results and discussion

Theoretical results of the inclusion process of Tetracaïne in β-CD

Since the inclusion process may take place on either side of the β-CD, a potential energy scan of the inclusion process is carried out through both sides of the guest molecule. Several mechanisms and orientations of the Tetracaïne may occur theoretically, either the $-N(CH_3)_2$ or the $-NH(C_4H_9)$ group may be oriented towards the primary or secondary face of the β-CD. According to the methodology described earlier [30, 31], a selective process of the insertion is observed and stable structures are obtained when the $-N(CH_3)_2$ group is included into the hydrophobic cavity of the β-CD (i. e. the primary face). The inclusion profile is reported in Fig. 2 (curve 'a'). We also found that the inclusion of the -$NH(C_4H_9)$ group can easily penetrate the β-CD from the secondary face. The potential energy profile of the insertion is reported in Fig. 2 (curve 'b').

All minima obtained in the potential energy profiles of the two insertion processes with the atoms of the β-CD frozen, are fully optimised with all variables free. Two minima P_{1a} and P_{2a} are observed for the insertion of the $-N(CH_3)_2$ group through the primary face, Fig. 2 (curve 'a'). The following results are obtained from a full optimization of these points at the Hartree–Fock level of theory with a 6-31G(d) basis set with a frequency analysis. For the insertion of the -$NH(C_4H_9)$ group from the secondary face, Fig. 2a (curve 'b'), two minima P_{1b} and P_{2b} are observed and the same approach is adopted. We shall refer to insertion process through the primary face as path (a) and through the secondary face path (b) leading to the 1:1 stoichiometry complex.

In order to evaluate the penetration depth, we have worked out the mean distance between hydrogen atoms of the $-N(CH_3)_2$ group (H–CH_3) and those of the $-NH(C_4H_9)$ group (H–CH_3), with the surrounding hydrogen's of type H3, H5 and H6 in the β-CD pointing towards the interior of the cavity. With these results we can safely conclude that an inclusion complex is formed with more details about the insertion level as shown in Fig. 2b. The mean distances for all the minima are reported in Table 1.

These results (Fig. 2b; Table 1), clearly show that the (H–CH_3) of the $-N(CH_3)_2$ group penetrates deep inside the host molecule and is close to hydrogen atoms of type H5 and H3. For the $-NH(C_4H_9)$ group, the distance shows that the (H–CH_3) is close to hydrogen of type H5. This observation indicate that the insertion of the $-N(CH3)_2$ group inside the primary face is deeper than the insertion of the $-NH(C_4H_9)$ group inside the secondary face of the β-CD. As the two processes are more likely to be competitive, we may suggest the hypothesis of a possible double insertion

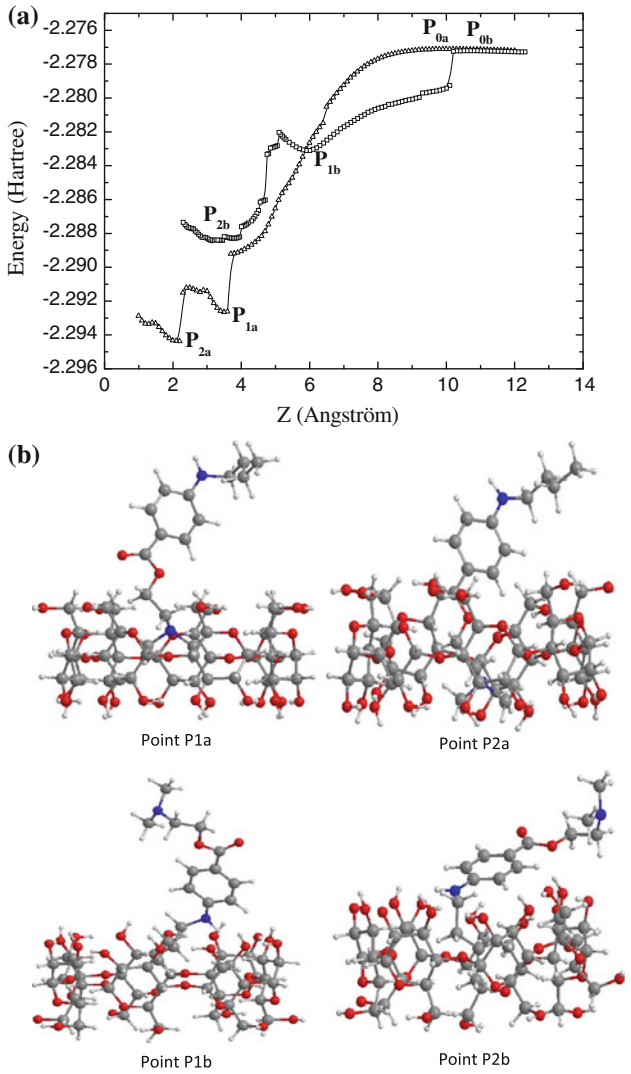

Fig. 2 **a** Potential energy profile of the inclusion of the $-N(CH_3)_2$ group of the Tetracaïn through the primary face (*open triangles* curve *a*) and the insertion through the secondary face of the $-NH(C_4H_9)$ group (*open squares* curve *b*). **b** Snapshots of the complex formation at different levels of the insertion, process path (**a**) refer to the insertion through the primary face (Point *1a* and Point *2a*) and path (**b**) refer to the insertion through the secondary face (Point *1b* and Point *2b*)

mechanism leading to 1:2 host–guest stoichiometry complex formations.

The calculated data of interest are reported in Table 2 for the $-N(CH_3)_2$ group inside the primary face (Fig. 2a, curve 'a') and for the insertion of the –NH (C_4H_9) group through the secondary face (Fig. 2a, curve 'b'). The insertion energy (or stabilization) within the supramolecular approach for the highest level of theory is calculated from the expression:

$$\Delta E = E_{AB} - (E_A + E_B). \quad (1)$$

where E_{AB} is the energy of the complex, and E_A and E_B are energies of monomers A and B. The deformation energy of

Table 1 Host–guest hydrogens mean distances for the minima obtained for the two type of insertion: $-N(CH_3)_2$ inside the primary face of the β-CD and –NH (C_4H_9) inside the secondary face of the β-CD

	Host hydrogen type		
	Primary face H3	Middle H5	Secondary face H6
Guest N $(CH_3)_2$			
(H–CH_3) 1st minimum (P_{1a})	6.16 Å	5.32 Å	6.51 Å
(H–CH_3) 2nd minimum (P_{2a})	5.24 Å	5.81 Å	6.81 Å
Guest NH (C_4H_9)			
(C_4H_9) 1st minimum (P_{1b})	4.01 Å	4.31 Å	6.58 Å
(C_4H_9) 2nd minimum (P_{2b})	6.31 Å	4.95 Å	5.86 Å

DE_X^{PTi} component X of the complex at point i, is calculated from the expression:

$$\Delta E_X^{PTi} = E_X^{PT0} - E_X^{PTi}. \quad (2)$$

All data are calculated with respect to the starting point (P_{0a} and P_{0b}). The reported data describe the binding energy of the host guest supramolecular system as a function of the penetration depth. The host–guest association is thermodynamically stable when compared to the separate state. At the HF level of theory, the deformation energy clearly shows that the guest molecule undergoes greater structural changes when compared to the host. This suggests that the guest molecule has to accommodate according to the penetration depth.

According to statistical thermodynamics, the stability constant of the association process may be related to the standard free energy by $\Delta G^0_{R,P}$

$$K_{R,P} = e^{-\left(\Delta G^0_{R,P}/RT\right)} \quad (3)$$

here, the indices R and P refer to the reactants and products of the association process respectively, R is the gas constant and T the absolute temperature (K).

$$R\ (\text{Reactant}) \rightarrow P\ (\text{Products}) \quad (4)$$

The standard free energy change can be $\Delta G^0_{R,P}$ written

$$\Delta G^0_{R,P} = \Delta E^o_{R,P} - T\Delta S^{vib(o)}_{R,P} \quad (5)$$

$$\text{With } \Delta E^0_{R,P} = \delta E^{elec}_{R,P} + \delta E^{vib(o)}_{R,P} \quad (6)$$

$$\text{and } \Delta S^{vib(0)}_{R,P} = S^{vib(o)}_R - S^{vib(o)}_P \quad (7)$$

Each term of Eq. 6 can be obtained from

$$\delta E^{elec}_{R,P} = E^{elec}_R - E^{elec}_P \quad (8)$$

$$\delta E^{vib(o)}_{R,P} = E^{vib(o)}_R - E^{vib(o)}_P \quad (9)$$

Table 2 Calculated properties at different insertion levels of the host–guest complexes for the two types of insertion at different levels of theory PM3 and HF calculations

Primary face complex (P0a, Pla, P2a)				Secondary face complex (P0b, P1b, P2b)		
PM3 calculation	Tetracaïne	β-CD	Complex	Tetracaïne	β-CD	Complex
Starting point (Poa, Pob)						
HOMO (eV)	−8.810	−10.822	−8.727	−8.810	−10.819	−8.885
LUMO (eV)	−0.320	+1.659	−0.210	−0.320	+1.661	−0.378
HOMO–LUMO gap (eV)	8.49	12.541	8.517	8.490	12.480	8.507
HOMO(Tet)–LUMO(cd) gap(eV)	10.469			10.471		
HOMO(cd)–LUMO(Tet)gap(eV)	10.502			10.499		
Interaction energy (Kcal/mol)	0.23			0.33		
1st minima (Pia, Pib)						
HOMO (eV)	−8.713	−10.815	−8.846	−8.809	−10.818	−9.078
LUMO (eV)	−0.193	+1.653	−0.383	−0.318	+1.654	−0.544
HOMO–LUMO gap (eV)	8.520	12.469	8.463	8.490	12.473	8.534
HOMO(Tet)–LUMO(CD) gap (eV)	10.366			10.463		
HOMO(CD)–LUMO(Tet) gap (eV)	10.622			10.500		
Interaction energy (Kcal/mol)	0.11			0.06		
Deformation energy of the (Kcal/mol)	0.006			0.006		
2nd minima (P2a, Pib)						
HOMO (eV)	−8.712	−10.816	−8.862	−8.805	−10.821	−9.085
LUMO (eV)	−0.192	+1.660	−0.429	−0.309	+1.654	−0.524
HOMO-LUMO gap (eV)	8.522	12.476	8.432	8.496	12.475	8.561
HOMO(Tet)-LUMO(CD) gap (eV)	10.372			10.45		
HOMO(CD)_LUMO(Tet) gap (eV)	10.620			10.512		
Interaction energy (Kcal/mol)	0.20			0.12		
Deformation energy (Kcal/mol)	0.01			0.03		
HF (6-31G (d)) Calculation						
Starting point (P_{0a}, P_{0b})						
HOMO (eV)	−7.657	−11.211	−8.207	−7.835	−11.214	−8.239
LUMO (eV)	+3.477	+5.442	+2.918	+3.315	+5.491	+2.831
HOMO-LUMO gap (eV)	1.134	16.653	11.125	11.15	16.705	11.071
HOMO(Tet)-LUMO(CD) gap (eV)	13.099			13.326		
HOMO(CD)-LUMO(Tet) gap (eV)	14.688			14.529		
Interaction energy (Kcal/mol)	−3.46			−6.61		
1st minima (Pia, Pib)						
HOMO (eV)	−7.756	−11.224	−8.218	−8.029	−11.102	−8.248
LUMO (eV)	+3.453	+5.431	+2.936	+3.247	+5.485	+2.813
HOMO-LUMO gap (eV)	11.209	16.655	11.154	11.276	16.587	11.061
HOMO(Tet)-LUMO(CD) gap (eV)	13.187			13.514		
HOMO(CD)-LUMO(Tet) gap (eV)	14.678			14.349		
Interaction energy (Kcal/mol)	0.38			0.631		
Deformation energy (Kcal/mol)	0.536			3.298		
2nd minima (Pia, Pib)						
HOMO (eV)	−7.836	−11.129	−8.336	−7.897	−11.223	−7.987
LUMO (eV)	+3.347	+5.496	+2.693	+3.311.217	+5.453	+3.038
HOMO-LUMO gap (eV)	11.183	16.625	11.029	20	16.676	11.025
HOMO(Tet)-LUMO(CD) gap (eV)	13.332			13.350		
HOMO(CD)-LUMO(Tet) gap (eV)	14.476			14.543		
Interaction energy (Kcal/mol)	0.13			0.27		

Table 2 continued

Primary face complex (P0a, Pla, P2a)				Secondary face complex (P0b, P1b, P2b)		
PM3 calculation	Tetracaïne	β-CD	Complex	Tetracaïne	β-CD	Complex
Deformation energy (Kcal/mol)	2.09			3.36		
Stability constant K_{RP}	3.5125E−3			2.2643E−5		

The input data necessary for the calculation of Eqs. 7, 8 and 9 are obtained from the optimisation and frequency calculation of the different points of the insertion process.

E_R^{elec} and E_P^{elec} are the minima of the potential energy surface (with the zero point energy),

$E_R^{vib(o)}$ and $E_P^{vib(o)}$ the zero point vibrational energy. $S_R^{vib(o)}$ and $S_P^{vib(o)}$ are the zero point vibronic entropy contribution of the reactants and product respectively.

The calculated association constants reported in Table 2 suggest that the association process occurs mainly through the primary face path (a) since $K_{R,p}^{FP} > K_{R,P}^{FS}$.

Despite the relative small deformation energies of the guest molecule and its structural changes, it could be of great interest to focus on the structure–activity relationship during the host guest insertion process. Despite the observed structural changes of the guest molecule, the properties are not substantially modified. In order to seek for any differences, the Fukui's indices according to the function f(r) as proposed by Parr and Yang [38], are worked out to explain the relative reactivity's of different sites in the molecule. To achieve such goal, we have implemented within the gamess [39] quantum chemistry program, the calculation of the Fukui's function written in its condensed form [40]:

$$f_k^{\alpha} = \sum^{AO} C_{\mu\alpha}^2 + \sum^{AO} C_{\gamma\alpha} C_{\mu\alpha} S_{\gamma\mu}. \tag{10}$$

The calculation is straightforward from the molecular frontier orbital coefficient $C_{\mu\alpha}$ and the atomic orbital overlap matrix $S_{\nu\mu}$. To avoid any unphysical data of the Fukui's function f_k^{α} (i.e. negative values) all single points calculations are performed at the HF level of theory followed by a Moller–Plesset [41] (MP2) correlation energy correction truncated at the second-order or followed by a configuration interaction (CI) with a 6-31G(d) basis set.

Other molecular descriptors such as the HOMO–LUMO gap $\Delta E_{HOMO-LUMO}$ (Eq. 11), the electronic chemical potential [38, 42] μ (Eq. 12), the global molecular hardness η [43] expressing the resistance to charge transfer (Eq. 13) and its inverse the global local softness S (Eq. 14), both expressed as a function of the ionization potential (IP) and the first electronic affinity (AE) of the neutral molecule or the corresponding E_{HOMO} and E_{LUMO} respectively according to the Koopmans theorem [44].

$$\Delta E_{HOMO-LUMO} = E_{HOMO} - E_{LUMO} \tag{11}$$

$$\mu \approx \frac{1}{2}[I + A] = \frac{1}{2}[E_{HOMO} + E_{LUMO}]. \tag{12}$$

$$\eta \approx \frac{1}{2}[I - A] = \frac{1}{2}[E_{LUMO} - E_{HOMO}]. \tag{13}$$

$$S \approx \frac{1}{\eta}. \tag{14}$$

The electrophilic power ω, defined as the energetic stabilization as a consequence of the charge transfer (Eq. 8) is.

$$\omega \approx \frac{\mu^2}{2\eta}. \tag{15}$$

From these data other properties such as local descriptors may be worked out. As an example, the local softnesses are related to the Fukui's indices by Eq. 16.

$$f = \eta S. \tag{16}$$

All these activity indicators are computed for the Tetracaïne in its equilibrium geometry (gas phase) and compared to that in the complexes at different insertion points of the potential energy profile. The atomic numbering of the Tetracaïne is reported in Fig. 1. The calculated molecular descriptors reported in Table 3 clearly show that the structural changes have no major influence on the properties of the guest molecule. We should underline that the N_{15} atom of the –NH(C_4H_9) group is the preferred site for protonation. The N_{15} atom is involved in inter-molecular hydrogen bonding with the oxygen atom of the β-CD. As a consequence of such interaction the Tetracaïne is stabilized which suggest that the inclusion from the secondary face of the –NH(C_4H_9) group in the gas phase is not deep. In the case of the insertion from the primary face, the –N(CH_3)$_2$ group goes deeper since such interaction is ignored because of the relative orientation. This observation is in agreement with the previous data reported in Tables 1 and 2.

Table 3 Fukui functions and molecular descriptors of the selected atoms for the Tetracaïne in the different states

Global descriptors	Isolated Tetracaïne				Tetracaïne Point 1a				Tetracaïne Point 2a			
	Hardness = 0.20613 Softness = 4.85140 Electrophilicity = 0.10306 Chemical potential = 0.20613 Electronigativity = −0.20613				Hardness = 0.20480 Softness = 4.88271 Electrophilicity = 0.10240 Chemical potential = 0.20480 Electronigativity = −0.20480				Hardness = 0.20402 Softness = 4.90143 Electrophilicity = 0.10201 Chemical potential = 0.20402 Electronigativity = −0.20402			
	$f^-(\mathbf{r})$	$f^+(\mathbf{r})$	$\mathbf{s(r)}^-$	$\mathbf{s(r)}^+$	$f^-(\mathbf{r})$	$f^+(\mathbf{r})$	$\mathbf{s(r)}^-$	$\mathbf{s(r)}^+$	$f^-(\mathbf{r})$	$f^+(\mathbf{r})$	$\mathbf{s(r)}^-$	$\mathbf{s(r)}^+$
N_1	0.00003	0.00001	0.00014	0.00003	0.00007	0.0003	0.00032	0.00016	0.00010	0.00013	0.00049	0.00065
C_4	0.00001	0.00003	0.00006	0.00012	0.00060	0.00081	0.00292	0.00397	0.00005	0.00006	0.00026	0.00031
O_6	0.00538	0.01773	0.02611	0.086602	0.00524	0.01805	0.02558	0.08813	0.00575	0.01886	0.02816	0.09244
C_7	0.00537	0.16074	0.02604	0.77980	0.00590	0.16223	0.02883	0.79212	0.00605	0.16597	0.02967	0.81348
O_8	0.03265	0.07894	0.15840	0.38295	0.03230	0.07515	0.15771	0.36693	0.03353	0.07924	0.16434	0.38839
C_9	**0.26462**	**0.15315**	**1.28380**	**0.74299**	**0.26547**	**0.14945**	**1.29622**	**0.72973**	**0.26544**	**0.14456**	**1.30102**	**0.70856**
C_{12}	**0.13573**	**0.01164**	**0.65850**	**0.05645**	**0.12231**	**0.24343**	**0.59719**	**1.18862**	**0.11817**	**0.24376**	**0.057919**	**1.19479**
N_{15}	**0.21450**	**0.03146**	**1.04061**	**0.15264**	**0.21974**	**0.03825**	**1.07293**	**0.18679**	**0.22159**	**0.03970**	**1.08611**	**0.19459**
C_{16}	0.00538	0.00286	0.02609	0.01388	0.00679	0.00084	0.03314	0.00412	0.00654	0.00097	0.03206	0.00476

Global descriptors	Tetracaïne Point 1b				Tetracaïne Point 2b			
	Hardness = 0.20579 Softness = 4.85922 Electrophilicity = 0.10290 Chemical potential = 0.20579 Electronigativity = −0.20579				Hardness = 0.20433 Softness = 4.89412 Electrophilicity = 0.10216 Chemical potential = 0.20433 Electronigativity = −0.20433			
	$f^-(\mathbf{r})$	$f^+(\mathbf{r})$	$\mathbf{s(r)}^-$	$\mathbf{s(r)}^+$	$f^-(\mathbf{r})$	$f^+(\mathbf{r})$	$\mathbf{s(r)}^-$	$\mathbf{s(r)}^+$
N_1	0.00003	0.00004	0.00014	0.00020	0.00006	0.00003	0.00027	0.00012
C_4	0.00004	0.00000	0.00021	0.00001	0.00008	0.00012	0.00038	0.00058
O_6	0.00517	0.01835	0.02511	0.08919	0.00539	0.01793	0.02640	0.08777
C_7	0.00527	0.16159	0.02563	0.78521	0.0060	0.16526	0.02935	0.80879
O_8	0.03378	0.07921	0.16416	0.38488	0.03224	0.07976	0.15780	0.39035
C_9	**0.26359**	**0.15318**	**1.28085**	**0.74431**	**0.26248**	**0.14680**	**1.28461**	**0.71846**
C_{12}	**0.13413**	**0.24003**	**0.65175**	**1.16636**	**0.11797**	**0.24043**	**0.57738**	**1.17671**
N_{15}	**0.21440**	**0.03301**	**1.04180**	**0.16042**	**0.22553**	**0.03876**	**1.10375**	**0.18971**
C_{16}	0.00782	0.00157	0.03802	0.00760	0.00677	0.00097	0.03315	0.00473

Data of nucleophilic or electrophilic sites are in bold

Raman spectra and theoretical data analysis

Raman spectroscopy is an efficient and accurate technique for identification and a qualitative analysis of drugs. It is often a hard and tough task to interpret and identify the spectroscopic data with no prior information at molecular scale. The purpose of this approach is to seek for a particular signature of the host–guest molecular complex when compared to its separate components. This is achieved by a theoretical calculation at the Hartree–Fock level of theory of the Raman spectra [37]. The calculated spectrum of the host–guest inclusion complex and its components is reported in Fig. 3 for the insertion of the $-N(CH_3)_2$ group from the primary face and Fig. 4 for the insertion of the $-NH(C_4H_9)$ from the secondary face. For both spectra, the second points (P_{2a} and P_{2b}) are considered as points of interest. Raman spectrum intensity of the β-CD is negligible when compared to that of the Tetracain except for the CH and OH stretching mode. Three regions can be described in terms of the frequencies as a primary signature of such complex molecular systems. The main stretching mode frequencies are identified and reported in the figures. We shall focus on the ν_{O-H}, of the hydroxyl group on both sides of the β-CD in the region (3,000–3,800 cm^{-1}) and the ν_{C-N}, ν_{N-H} of the Tetracaïne in the region lying between 2,700 and 3,700 cm^{-1}. The former, which describes the vibrational mode of the hydrogen bonding network on both sides of the β-CD, should give us some details on the transformations undertaken by the host. On the other side, ν_{N-H} describe the vibrational mode of the NH group of the guest molecule and ν_{C-H} vibrational mode of the C–H bond particularly those in the $-N(CH_3)_2$, $-NH(C_4H_9)$ group and

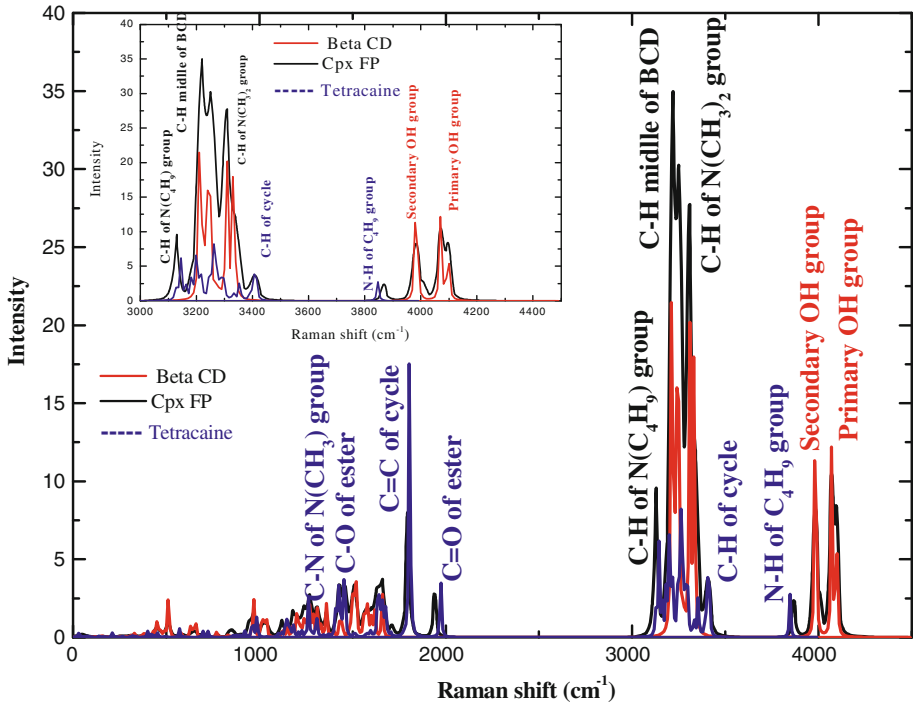

Fig. 3 Superposition of the theoretical Raman spectra for the inclusion complex (P_{2a}) from the primary face and its components

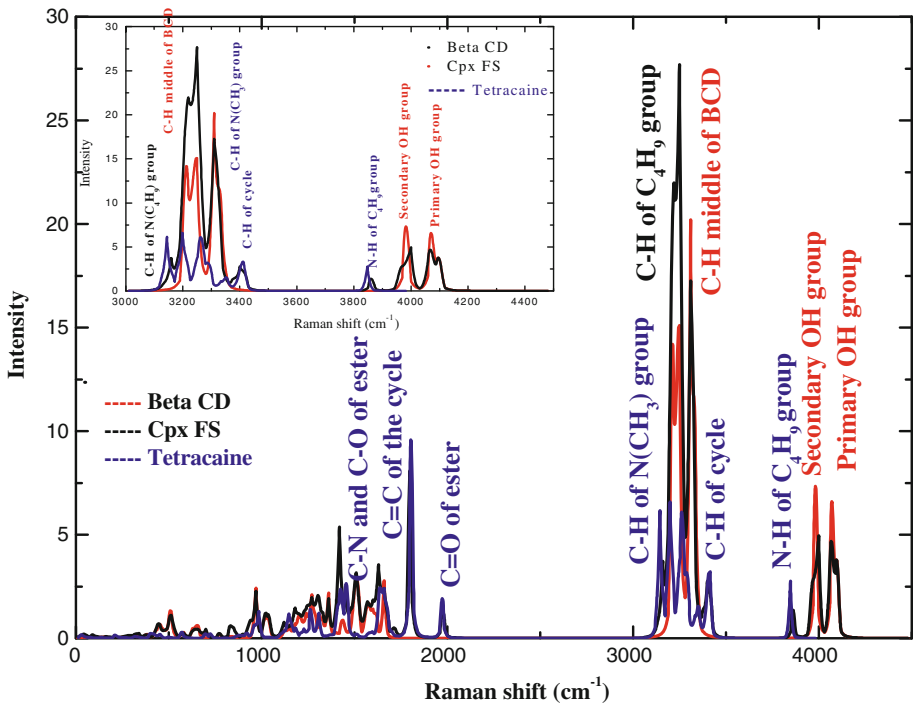

Fig. 4 Superposition of the theoretical Raman spectra for the inclusion complex (P_{2b}) from the secondary face and its components

the hydrogen's in the middle of the β-CD and the phenyl ring.

The influence of the molecular ratio Tetracain/β-CD on the shape of the spectra is shown in Figs. 5 (Tetracain concentration in excess) and 6 (β-CD concentration in excess). For equimolar concentrations the Raman spectra (Fig. 5.) of both components is conserved. The OH vibrational band (3,100–3,500 cm^{-1}) and NH vibrational peak (3,387 cm^{-1}) are conserved with a lower intensity. The band structure of the CH stretching modes for the two molecular species is modified for the equimolar mixture. These observations suggest that the inclusion complex has taken place and that the host molecular system does not undergo any structural changes. At higher Tetracain mol

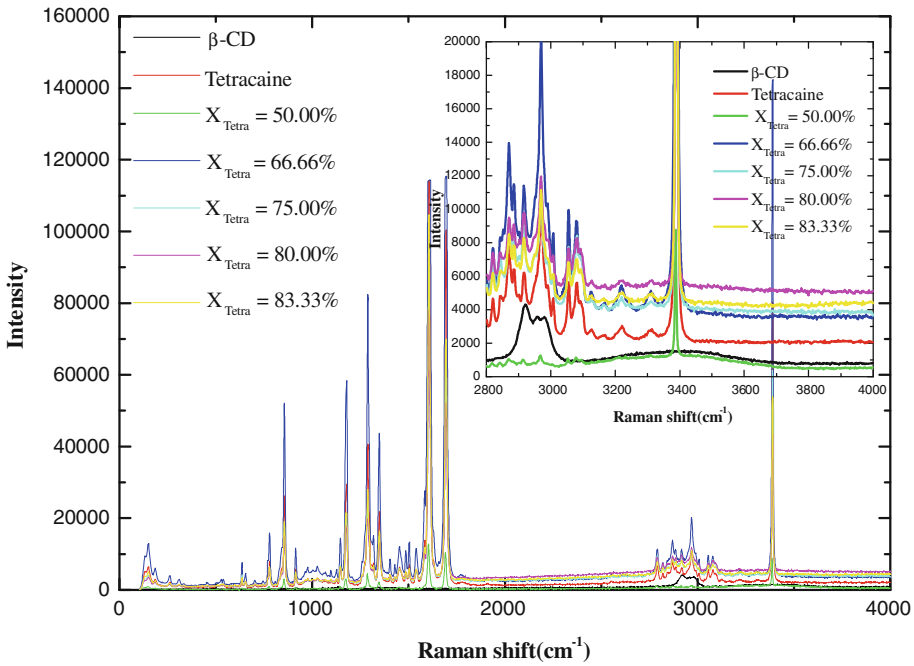

Fig. 5 Experimental Raman spectrum of the mixture Tetracain/β-CD at different mol fraction of the Tetracain

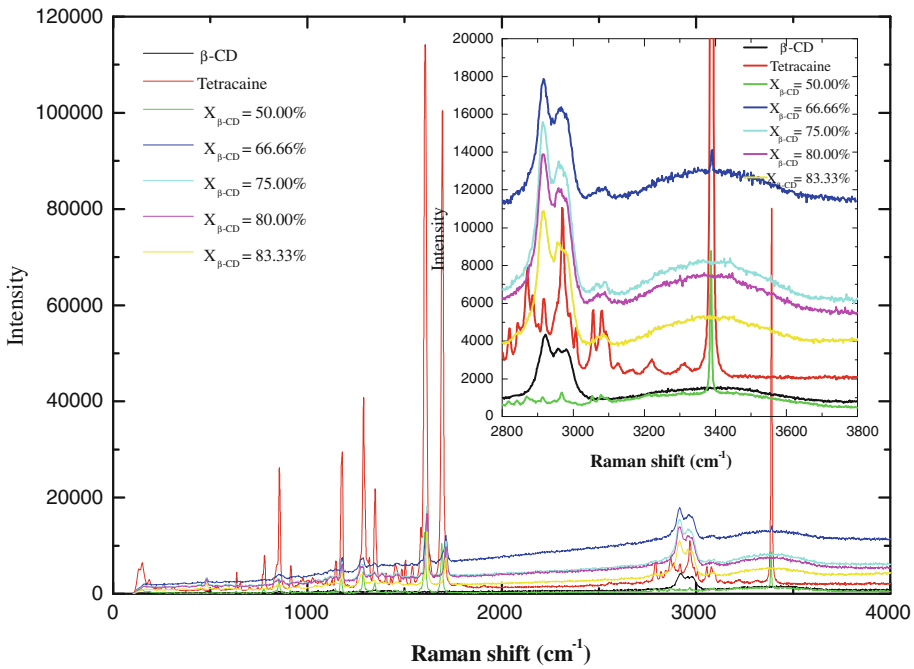

Fig. 6 Experimental Raman spectrum of the mixture Tetracain/β-CD at different mol fraction of the β-CD

ratio, the N–H and O–H stretching mode appears as a high intensity peak, the hydrogen bond rim is not observed; this suggests that a saturated molecular inclusion complex has been reached. Similar observations are made when the β-CD is in excess (Fig. 6.), the band structure of the O–H stretching mode for the host molecule is maintained at high mol ratio of the β-CD.

The Raman spectra of the C–H stretching mode of the β-CD ($X_{\beta\text{-CD}} = 100\%$) and the Tetracain/$\beta$-CD mixture ($X_{\beta\text{-CD}} = 50\%$) is shown in Fig. 7. An asymmetric central band with two shoulders is observed. These Raman spectra can only be successfully fitted by three components (Lorentzian functions). The fitted frequency values are 2919.93, 2960.03 and 2984.7 cm^{-1} and correspond to the three types of hydrogen's (H3, H5 and H6) within the β-CD that might undergo a perturbation during the insertion process. This behavior of the C–H stretching mode for the β-CD is reproducible for the mixture, but the intensity

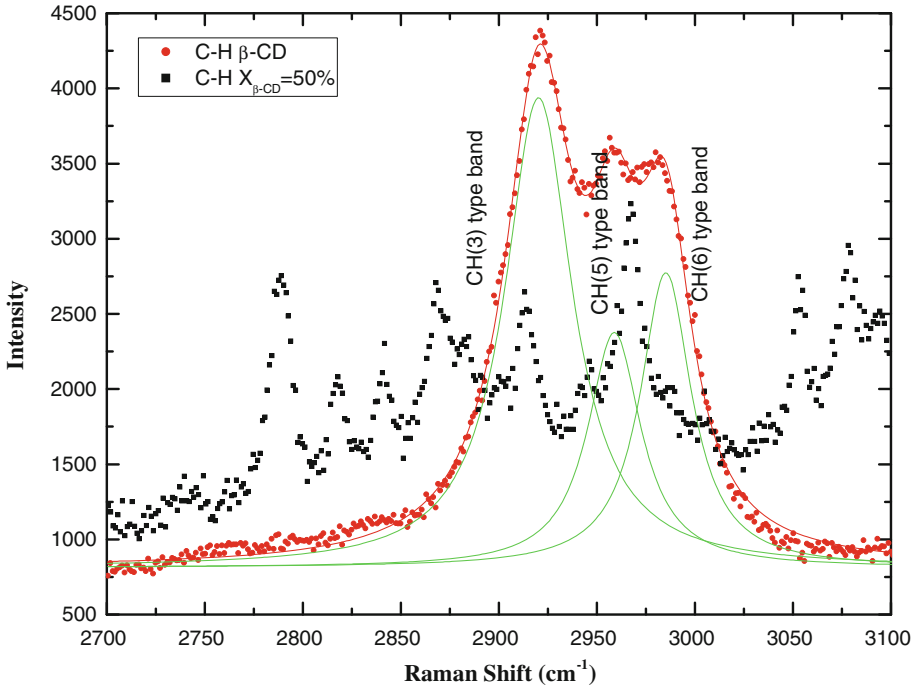

Fig. 7 Raman spectra of the C–H stretching mode of the β-CD ($X_{\beta\text{-CD}} = 100\%$) and the Tetracain/$\beta$-CD mixture ($X_{\beta\text{-CD}} = 50\%$). The *solid lines* represent the three C–H types of the β-CD components fitted by Lorentzian functions

of each of the four components changes considerably. This phenomenon could be explained by the influence of the guest molecules. The changes observed on the C–H(3) type band (Secondary face) suggest that the insertion occurs mainly from the secondary face in perfect agreement with the our theoretical assumption.

Conclusion

The interactions between drug molecules and cyclodextrins constitute the key research problem for drug research and such interactions can sometimes be difficult to master directly by theoretical calculations. The particular signature of host–guest complexes can be observed by Raman spectroscopy with the help of quantum mechanical approaches at a high level of theory. Quantum chemistry and the molecular descriptors are useful tools to describe the potential energy surface of the insertion processes and identify the final insertion host–guest complex most likely to occur. Although, the guest molecule undergoes relative important structural changes, when compared to the host, no major differences in its properties are observed. For more accurate results, the calculation of the molecular descriptors should be carried out on the whole host–guest supramolecular system, to confirm such hypothesis. For more reliable results and avoid unphysical data, the Fukui's indices and molecular descriptor should be worked out at the HF level of theory followed by a single point Moller–Plesset [41] (MP2) correlation energy correction truncated at the second-order or followed by a configuration interaction (CI) and with a 6-31G(d) basis set.

This work is dedicated to our friend and colleague Pr. D. Bormann (Laboratoire Condition Extrémes et Matériaux: Haute Temperature et Irradiation, CEMHTI, CNRS Orleans, France), who passed away in summer 2009.

Acknowledgments The authors are deeply grateful to Pr. M. dauchez and the University of Reims Champagne Ardennes (URCA, France) for computing resources and computer time used on romeo calculator, as we are deeply grateful to Pr. P. Simon and the Laboratoire Condition Extrémes et Matériaux: Haute Temperature et Irradiation, CEMHTI (CNRS Orleans, France) for spectroscopy facilities and support.

References

1. Connors, K.A.: The stability of cyclodextrin complexes in solution. Chem. Rev. **97**, 1325 (1997)
2. D'Souza, V.T., Lipkowitz, K.B.: Cyclodextrins: introduction. Chem. Rev. **98**, 1741 (1998)
3. Sun, X.Q., Meng, Q., Yan, H.B.: Introduction of supermolecular chemistry, p. 11. Chinese Petrochemistry Press, Beijing (1997)
4. Loftsson, T., Brewster, M.E.: Pharmaceutical applications of cyclodextrins. J. Pharm. Sci. **85**(10), 1017 (1996)
5. Gellman, S.H.: Introduction: molecular recognition. Chem. Rev. **97**, 1231 (1997)
6. Breslow, R., Dong, S.D.: Biomimetic reactions catalyzed by cyclodextrins and their derivatives. Chem. Rev. **98**, 1997 (1998)
7. Hamilton, J.A., Sabesan, M.N.: Structure of inclusion complexes of cyclomaltoheptaose (cycloheptaamylose): crystal structure of the benzocaine adduct. Carbohydr. Res. **102**, 31 (1982)
8. Uekama, K., Hirayama, F., Irie, T.: Cyclodextrin drug carrier systems. Chem. Rev. **98**, 2045 (1998)

9. Caliceta, P., Salmaso, S., Semenzato, A., Carofiglio, T., Fornasier, R., Fermeglia, M., Ferrone, M., Pricl, S.: Synthesis and physicochemical characterization of folate-cyclodextrin bioconjugate for active drug delivery. Bioconjug. Chem. **14**, 899 (2003)
10. Djedaini, F., Perly, B.: Organic shift reagents for the NMR analysis of cyclodextrins. J. Mol. Struct. **239**, 161 (1990)
11. Szente, L., Szejtli, J.: Non-chromatographic analytical uses of cyclodextrins. Analyst **123**, 735 (1998)
12. Frömming, K.-H., Szejtl, J.: Cyclodextrin in pharmacy: topics in inclusion science. Kluwer Academic Publishers, The Netherland (1994)
13. Uekama, K., Fujinaga, T., Hirayama, F., Otagiri, M., Yamasaki, M.: Inclusion complexations of steroid hormones with cyclodextrins in water and in solid phase. Int. J. Pharm. **10**, 1 (1982)
14. Kang, J., Kumar, V., Yang, D., Chowdhury, P.R., Hohl, R.J.: Cyclodextrin complexation: influence on the solubility, stability, and cytotoxicity of camptothecin, an antineoplastic agent. Eur. J. Pharm. Sci. **15**, 163 (2002)
15. Li, N., Zhang, Y.H., Xiong, X.L., Li, Z.G., Jin, H.H., Wu, Y.N.: Study of the physicochemical properties of trimethoprim with beta-cyclodextrin in solution. J. Pharm. Biomed. Anal. **38**, 370 (2005)
16. Brewster, M.E., Loftsson, T.: Cyclodextrins as pharmaceutical solubilizers. Adv. Drug Deliv. Rev. **59**, 645 (2007)
17. Bowman, W.C., Rand, M.J.: Textbook of pharmacology. Blackwell, Cambridge (1990)
18. Avendaño, C.: Introducción a la Química FarmacéUtica. McGraw-Hill Interamaricana, Madrid (1993)
19. Qin, W., Jiao, Z., Zhong, M., Shi, X.J., Zhang, J., Li, Z., Cui, X.: Simultaneous determination of procaine, lidocaine, ropivacaine, tetracaine and bupivacaine in human plasma by high-performance liquid chromatography. J. Chromatogr. B Anal. Technol. Biomed. Life Sci. **15-16**, 1185 (2010)
20. Atwood, J.L., Davies, J.E.D., MacNicol, D.D., Vögtle, F.: Comprehensive supramolecular chemistry. Pergamon, Oxford (1996)
21. Schneider, H.J., Hacket, F., Rüdiger, V., Ikeda, H.: NMR studies of cyclodextrins and cyclodextrin complexes. Chem. Rev. **98**, 1755 (1998)
22. Harata, K.: Structural aspects of stereodifferentiation in the solid state. Chem. Rev. **98**, 1803 (1998)
23. Liu, L., Xiao-Song, L., Song, K.-S., Guo, Q.-X.: PM3 studies on the complexation of α-cyclodextrin with benzaldehyde and acetophenone. J. Mol. Struct. Theochem **531**, 127 (2000)
24. Li, X., Liu, L., Guo, Q.X., Chu, S.D., Liu, YC. PM3 molecular orbital calculations on the complexation of alpha-cyclodextrin with acetophenone. Chem. Phys. Lett. 307 (1999)
25. Li, X., Liu, L., Mu, T.W., Guo, Q.X. A Systematic Quantum Chemistry Study on Cyclodextrins. Monatsh. Chem. 131 (2000)
26. Liu, L., Li, X., Guo, Q.X., Liu, Y.C.: Hartree–Fock and density functional theory studies on the molecular recognition of the cyclodextrin. Hartree–Fock and density functional theory studies on the molecular recognition of the cyclodextrin. Chin. Chem. Lett. **10**, 1053 (1999)
27. Yang, E.-C., Zhao, X.-J., Hua, F., Hao, J.-K.: Semi-empirical PM3 study upon the complexation of β-cyclodextrin with 4,4′-benzidine and *o*-tolidine. J. Mol. Struct. Theochem **712**, 75 (2004)
28. Yan, C., Xiaohui, L., Xiu, Z., Hao, C.: A quantum-mechanical study on the complexation of β-cyclodextrin with quercetin. J. Mol. Struct. Theochem. **764**, 95 (2006)
29. Yan, C.L., Xiu, Z.L., Li, X.H., Hao, C.: Molecular modeling study of β-cyclodextrin complexes with (+)-catechin and (−)-epicatechin. J. Mol. Graph. Modelling **26**, 420 (2007)
30. Blidi Boukamel, N., Krallafa, A., Bormann, D., Caron, L., Canipelle, M., Tilloy, S., Monflier, E. Theoretical investigations of inclusion processes of (4-tert-butylphenyl)(3-sulfonatophenyl)(phenyl) phosphine in the β-cyclodextrin. J. Incl. Phenom. Macrocycl. Chem. **42** 269 (2002)
31. Chekirou, N.L., Krallafa, A., Bormann, D.: Theoretical investigations and mechanisms of the inclusion processes of bi(3-sulfonatophenyl) (4-tert-butylphenyl) phosphine in the beta-cyclodextrin. J. Incl. Phenom. Macrocycl. Chem. **53**, 89 (2005)
32. Stewart, J.J.P.: Optimization of parameters for semi-empirical methods I-method. J. Comp. Chem. **10**, 209 (1989)
33. Song, K.-S., Hou, C.-R., Liu, L., Xiao-Song, L., Guo, Q.-X.: A quantum-chemical study on the molecular recognition of β-cyclodextrin with ground and excited xanthones. J. Photochem. Photobiol. A Chem. **139**, 105 (2001)
34. Bugay, D.E.: Characterization of the solid-state: spectroscopic techniques. Adv. Drug Deliv. Rev. **48**, 43 (2001)
35. Johansson, J., Pettersson, S., Taylor, L.S.: Infrared imaging of laser-induced heating during Raman spectroscopy of pharmaceutical solids. J. Pharm. Biomed. Anal. **30**, 1223 (2002)
36. Bondesson, L., Mikkelsen, K.V., Luo, Y., Garberg, P., Agren, H.: Hydrogen bonding effects on infrared and Raman spectra of drug molecules. Spectrochim. Acta A Mol. Biomol. Spectrosc. **66**, 213 (2007)
37. Frisch, M.J., Trucks, G.W., Schlegel, H.B., Scuseria, G.E., Robb, M.A., Cheeseman, J.R., Montgomery, J.A. Jr., Vreven, T., Kudin, K.N., Burant, J.C., Millam, J.M., Iyengar, S.S., Tomasi, J., Barone, V., Mennucci, B., Cossi, M., Scalmani, G., Rega, N., Petersson, G.A., Nakatsuji, H., Hada, M., Ehara, M., Toyota, K., Fukuda, R., Hasegawa, J., Ishida, M., Nakajima, T., Honda, Y., Kitao, O., Nakai, H., Klene, M., Li, X., Knox, J.E., Hratchian, H.P., Cross, J.B., Adamo, C., Jaramillo, J., Gomperts, R., Stratmann, R.E., Yazyev, O., Austin, A.J., Cammi, R., Pomelli, C., Ochterski, J.W., Ayala, P.Y., Morokuma, K., Voth, G.A. , Salvador, P., Dannenberg, J.J., Zakrzewski, V.G., Dapprich, S., Daniels, A.D., Strain, M.C., Farkas, O., Malick, D.K., Rabuck, A.D., Raghavachari, K., Foresman, J.B., Ortiz, J.V., Cui, Q., Baboul, A.G., Clifford, S., Cioslowski, J., Stefanov, B.B., Liu, G., Liashenko, A., Piskorz, P., Komaromi, I., Martin, R.L., Fox, D.J., Keith, T., Al_Laham, M.A., Peng, C.Y., Nanayakkara, A., Challacombe, M., Gill, P.M.W., Johnson, B., Chen, W., Wong, M.W., Gonzalez, C., Pople, J.A. GAUSSIAN03, Revision C.02, Gaussian, Inc., Pittsburgh (PA) 2003
38. Parr, R.G., Yang, W.: Density functional theory of atoms and molecules. Oxford University Press, New York (1989)
39. Schmidt, M.W., Baldridge, K.K., Boatz, J.A., Elbert, S.T., Gordon, M.S., Jensen, J.H., Koseki, S., Matsunaga, N., Nguyen, K.A., Su, S.J., Windus, T.L., Dupuis, M., Montgomery, J.A.: GAMESS: general atomic and molecular electronic structure system. J. Comput. Chem. **14**, 1347 (1993)
40. Contreras, R.R., Fuentealba, P., Galvan, M., Perez, P.: A simple formalism devised to calculate the condensed-to-atoms Fukui function. Chem. Phys. Lett. **304**, 405 (1999)
41. Moller, C., Plesset, M.S.: Note on an approximation treatment for many-electron systems. Phy. Rev. **46**, 618 (1934)
42. Geerlings, P., De Proft, F., Langenaeker, W.: Conceptual density functional theory. Chem. Rev. **103**, 1793 (2003)
43. Pearson, R.G.: Chemical hardness: applications from molecules to solids. Wiley-VCH Verlag GMBH, Weinheim (1997)
44. Koopmans, T.A.: Über die Zuordnung von Wellenfunktionen und Eigenwerten zu den Einzelnen Elektronen Eines Atoms. Physica **1**, 104 (1934)